PROCEEDINGS, 41st Workshop on Geothermal Reservoir Engineering
Stanford University, Stanford, California, February 22-24, 2016
SGP-TR-209

Play Fairway Analysis for Structurally Controlled Geothermal Systems in the Central Cascades Arc-Backarc Regime, Oregon

Philip E. Wannamaker[1], Andrew J. Meigs[2], John D. Trimble[2], Ellen A. Lamont[2], B. Mack Kennedy[3], Joseph N. Moore1, Virginie Maris[1], Eric L. Sonnenthal[3] and Gregory D. Nash[1]

[1]University of Utah/Energy & Geoscience Institute, 423 Wakara Way, Ste 300, Salt Lake City, UT 84108 USA
[2]Oregon State University/College of Earth, Ocean and Atmospheric Sciences, 101 SW 26th St, Corvallis, OR 97331 USA
[3]Lawrence Berkeley National Laboratory, Earth Sciences Division, 1 Cyclotron Rd, Berkeley, CA 94720 USA

pewanna@egi.utah.edu

Keywords: play fairway analysis, central Cascades Oregon, exploration, GIS

ABSTRACT

A research team with membership from the University of Utah/EGI, the Oregon State University, and Lawrence Berkeley National Laboratory have carried out a play fairway analysis (PFA) for geothermal resources in the Central Cascades arc-backarc volcano-tectonic regime of central Oregon. This is a unique region for geothermal exploration because active Basin and Range (B&R) extension is superimposed upon and contemporaneous with subduction arc magmatism. Cumulative heat flow along the N-S strike grows from negligible values at the north end to >300 MW in the space of ~100 km concentrated in the northern portion of the PFA area. Perhaps surprisingly then, no geothermal resources leading to construction of an electricity-producing power plant have yet been identified in the U.S. Cascades. Succinctly, our PFA adds to understanding of the potential sources of heat and permeability in the region, which are the two principal criteria for establishing a geothermal resource. A constraint of the PFA project was that only existing data could be analysed, albeit using new and state-of-the-art methods. A challenge in this PFA region is the paucity of existing data, presumably related to the lack of historical geothermal development as well as some non-trivial access.

Criteria selected for establishing heat potential include direct heat flow measurements in boreholes, magnetotelluric (MT) low resistivity anomalies, fluid geochemistry, and proximity to recent volcanic eruptions. Permeability is established by fault density, propensity of faulted sub-regions for slip or dilation, and MT low resistivity anomalies. Heat source and permeability potential are expressed in terms of their individual common risk segment maps, with a color scheme using green for most favorable (low risk) and red for least favorable (high risk). Due to data scarcity, we need to mix approaches based upon probability kriging and conceptual global models based on experience in other environments. For dominantly andesitic arc type resources, inferred heat sources and permeability as well as land and transmission access suggest that prospective areas may lie along a NW-SE fault trend passing from Breitenbush Hot Springs area through the Mt Jefferson volcanic edifice into the backarc area, as well possibly as areas nearby to the north of Mt Jefferson. For dominantly extensional type resources, new areas worth examining could lie along diffusely oriented normal faulting extending north of Newberry volcano and into the Warm Springs region.

1. INTRODUCTION

Play Fairway Analysis (PFA) in the geothermal context combines regional geological/ geophysical understanding with knowledge of prospect control elements (e.g., origin of heat, pathways to heat up and concentrate fluids)to produce an inventory of prospect leads (see Fraser, 2010, for an oil and gas analog). The potential for new discoveries should be increased dramatically in regions where active magmatism creating a large heat endowment occurs in conjunction with diverse structural trends some of which may be well oriented to create reservoir space. Thus we have been drawn to examine the active central Cascades arc-backarc regime of central Oregon for favorable plays. Here, active Basin and Range (B&R) extension is superimposed upon and contemporaneous with subduction arc magmatism (Schmidt et al., 2008; Ingebritson and Mariner, 2010; Wannamaker et al., 2014) (Figure 1).

Our approach to reassessing geothermal resource potential in this region emphasizes application of MT geophysics, fluid geochemistry and structural geology to resolve heat source and permeability. The approach incorporates heat flow, volcanic distributions, multi-component geochemistry, and geothermal system modeling from a global context. It draws upon our experience in the extensional Great Basin where producing geothermal systems are characterized by crustal-scale, low electrical resistivity roots resolved from MT surveying that connect to deep magmatic activity (Wannamaker et al., 2007, 2011; Siler et al., 2014). Such systems lie also in favorably dilatent structural settings and appear to have isotopic compositions (He, O, C) indicative of deep high-T input. We also draw on our experience in andesitic volcanic systems in Central America, the Philippines and Indonesia (Moore et al., 2008; Raharjo et al., 2010).

A primary challenge in the project was the relative sparsity of data to analyse, which makes difficult a fully statistical analysis of existing data with uncertainty limits stemming from an established probability distribution. We will illustrate the extent to which statistical surfaces of individual data sets can be defined using the most densely sampled data sets in the region, heat flow and fault density. The priority exploration areas offered later in this report are derived both from statistically-based criteria functions and from conceptually-based global models focused by existing data in the PFA area. Multi-criteria decision making methods (MCDM) are examined to prioritize data sets and play fairway subregions. A large emphasis in the conclusions of the project is on recommendations for new data followup to identify new play areas.

2. BACKGROUND AND ASSUMPTIONS

Subduction zone volcanic arcs and continental extensional provinces represent the two most pro-ductive settings of exploitable geothermal resources (Ingebritson and Mariner, 2010; King and Metcalf, 2013). Central Cascadia should be a uniquely promising subregion for geothermal exploration because active Basin and Range (B&R) extension is superimposed upon and contemporaneous with subduction arc magmatism (Schmidt et al., 2008; Ingebritson and Mariner, 2010; Wannamaker et al., 2014) (Figure 1). Thus, the volcanic arc segment and its near backarc should be prospective in play fairway analysis (PFA) for structurally controlled, hydrothermal high-temperature, low-temperature and EGS geothermal resources. Despite the setting, there are no electricity power-producing geothermal systems in the U.S. Cascades. This can be ascribed to a combination of cryptic surface manifestations and sometimes difficult land access. Our project re-examines these issues and recommends followup exploration.

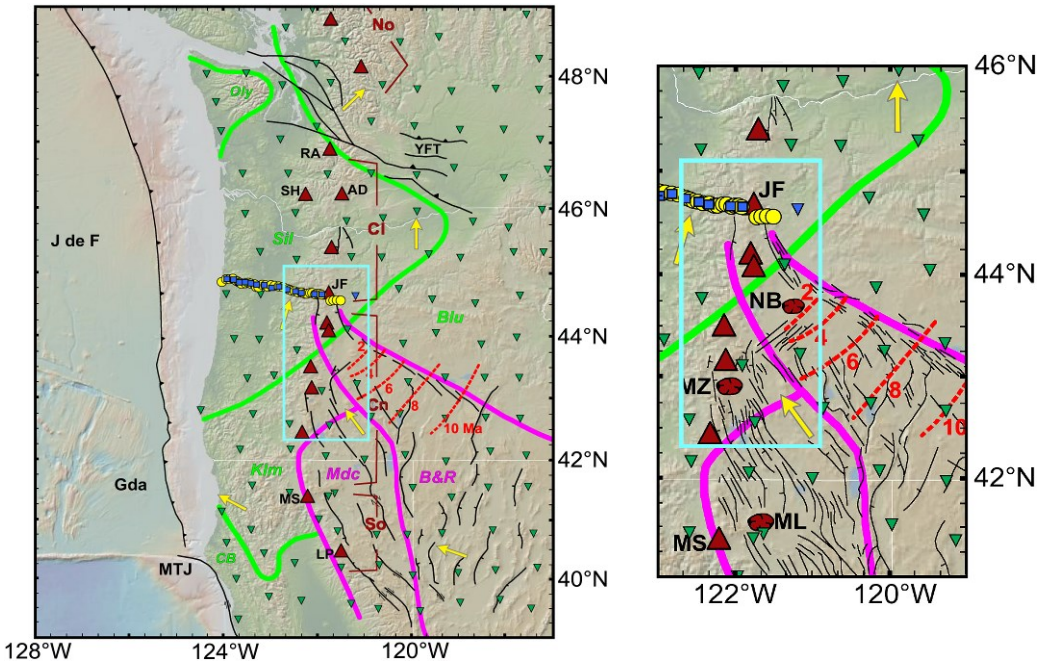

Figure 1: Location maps showing the play fairway analysis project area (cyan insets) modified after Wannamaker et al. (2014). Left (a): GPS geodetic motion estimate arrows are yellow, and contours of rhyolitic volcanism approaching the Central Cascades are red dashes (Hildreth, 2007). Green bands enclose terranes Siletzia, Klamath and Blue Mtns and Olympic Mtns. Pink bands enclose active terranes, Basin & Range and Modoc Plateau. Mt Jefferson is JF. Volcanic chain segment boundaries after Schmidt et al. (2008). Right (b): Enlargement shows faulting in more detail, plus Newberry (NB), Mt Mazama (MZ) and Medicine Lake (ML) volcanic centers. The EMSLAB MT transect is yellow circles and blue squares, and Earthscope MT transportable array (TA) stations are inverted green triangles.

The Central Cascades region could have heat sources and permeability of both subduction arc and extensional tectonism regimes. Simplified depictions of each type are redrawn from Henley and Ellis (1983) in Figure 3. In arc systems, a central intrusive edifice is the principal heat source. Induced circulating fluids tend to be neutral pH and Cl bearing with modest salinity (1-2 wt %). Examples of such fluids probably are those emerging along the High-Western Cascades boundary faults such as Breitenbush and Bigelow Hot Springs (Jefferson et al., 2006). High temperature NaCl reservoirs may lie in propylitic-grade rocks at 2-3 km, with lower-grade clay rich cap rocks above often constituting an electrical geophysical target (e.g., Moore et al., 2008). However, due to commonly steep slopes, shallow fluids can flow down slope for great distances, often over 10 km, frequently masking the presence of the underlying NaCl waters and even the clay cap. This is exacerbated by commonly dense vegetation cover, Cascades included. Such factors presumably contributed to the unsuccessful SUNEDCO 58-28 well drilled ~13 km NW of Mt Jefferson, or 3 km SE of Breitenbush Hot Springs (Sherrod, 1988). However, a high-temperature system may be hidden under the west flank of Three Sisters volcano as inferred by high ^{3}He flux through surface waters (Evans et al., 2004), and such a situation could exist elsewhere in this region as we will discuss.

In extension (rift) geothermal systems, uplift and exhumation of the crust elevates the geotherm and creates fracture permeability. A common model for geothermal systems here involves deep circulation of waters driven by topographic flow to depths potentially of 10 km near the brittle-ductile lithologic transition (Wisian and Blackwell, 2004; McKenna and Blackwell, 2004). Other high temperature extensional systems clearly have magmatic affinities given nearby volcanism and other evidence (e.g., Simmons et al., 2015). Fluid compositions similar to the andesitic setting can occur distal to the heat source in rift systems. Extension is key for making space to allow heat sources to upwell and for permeability to be created for geothermal fluids. It is considered responsible for the large and

abrupt increase in heat flow beginning between Mt Hood and Mt Jefferson at the north end of our PFA area and continuing to the south. Ingebritson and Mariner (2010) compute that approximately 300 MW of heat output occurs in the Mt Jefferson area alone (Figure 4).

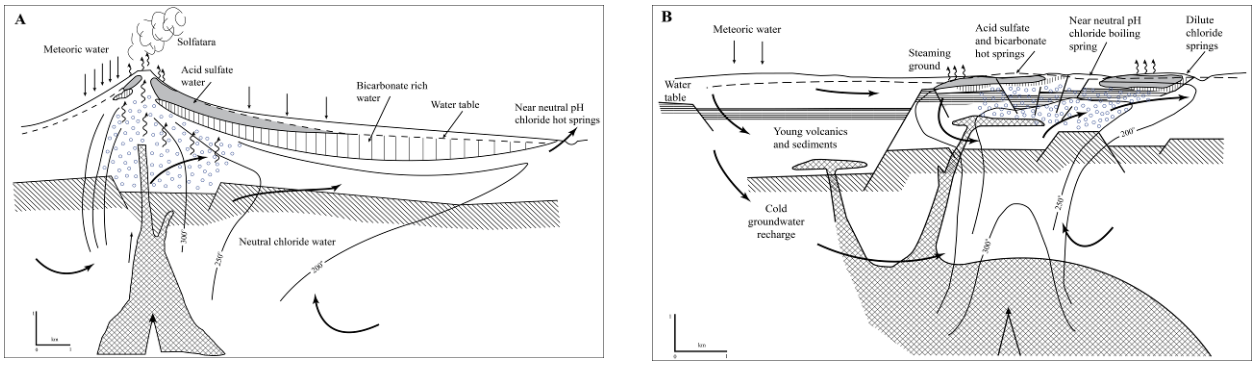

Figure 2: Schematic illustrations of andesitic (left) and rift (right) geothermal systems, after Henley and Ellis (1983).

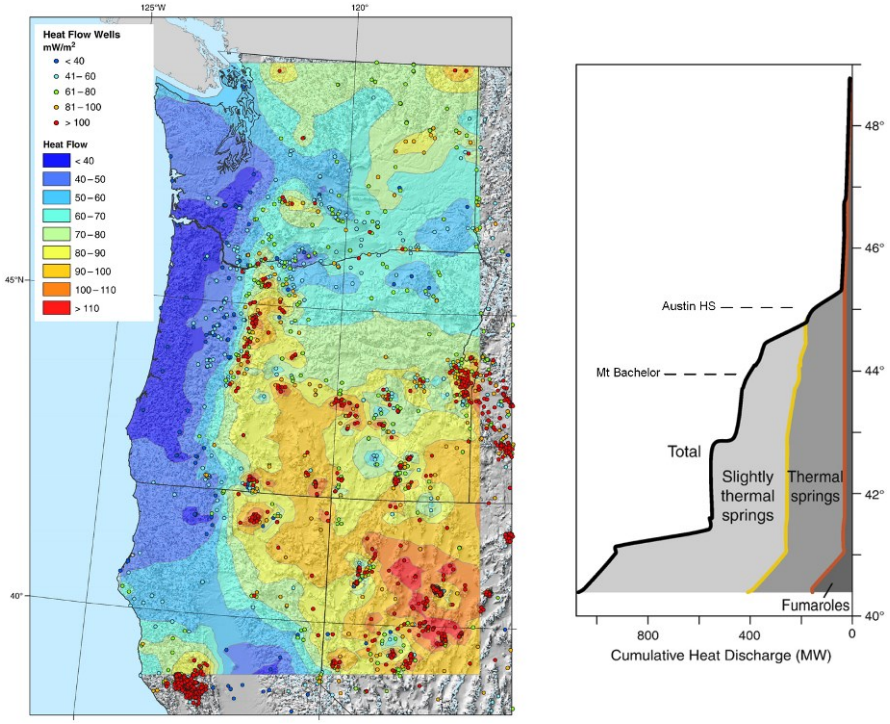

Figure 3: Left: Heat flow contour map of the northwestern U.S. Right: Cumulative heat flow discharge from Cascade Range hydrothermal features (summed north to south) showing that <5% of the total hydrothermal discharge occurs north of 45.15 deg N latitude. From Ingebritsen and Mariner (2010).

We modernize understanding of geothermal prospectivity of the Central Cascades by emphasizing a combination of magnetotellurics (MT), structural geology, and fluid chemistry integrated in a context of heat flow and volcanology. High-temperature geothermal systems in the Great Basin including Dixie Valley and McGinness Hills show MT low-resistivity roots connecting to probable magmatic underplating and fluid release in the deep crust (Wannamaker et al., 2007, 2011, 2013a,b) (Figure 2). The Great Basin studies also showed that high-temperature systems lie in structural geological settings favorable for dilatency. The Dixie Valley and McGinness Hills systems also exhibited elevated 3He content in sampled fluids confirming mantle magmatic geochemical contributions suggested by the MT resistivity structure. Thus, such low-resistivity roots are interpreted to represent large-scale permeability and potential heat upwelling. Related underplating and uprise of melts or fluids higher in the crust are inferred from 2D modeling of MT profiles across

the Cascades as well (Wannamaker et al., 2014). Thus the three methods of MT, structural geology, and fluid geochemistry will be combined in our study to infer the likeliest zones of high-temperature upwelling into favorable structural situations.

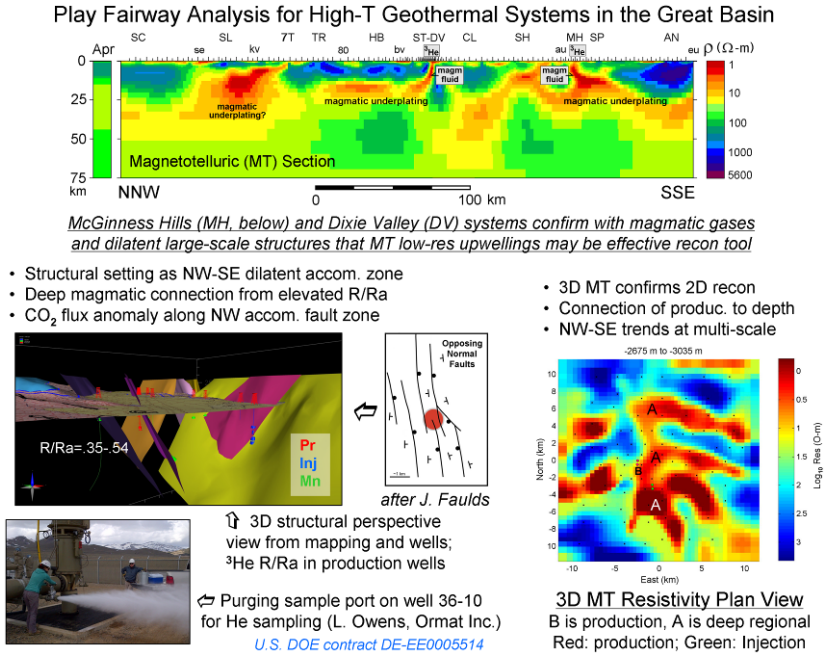

Figure 4: Illustration of integrative interpretation of the McGinness Hills NV moderate temperature geothermal system. Regional MT transect studies (top) uncovered several low-resistivity bodies in the deep crust ascribed to magmatic underplating and hydrothermal fluid release. Such systems in turn lie in 3D structural zones promoting dilatency. Sampled fluids show isotopic compositions confirming magmatic input. Study by Wannamaker et al. (2013b).

Even though data are relatively sparse in the central Cascades PFA area, we believe useful common risk segment maps of heat source and permeability can be derived. Ideally, risk distributions would be computed from a family of spatially continuous inputs represented in the depicted flow diagram. We will discuss which inputs are sufficiently sampled to derive a probability function and which simply can be concept-supporting. Drilling recommendations were not in the scope of Phase I, but solid suggestions for the collection of new data toward thermal gradient assessment are possible.

3. WORKFLOW AND RESULTS

At the outset, pertinent data to do PFA were assembled for the Central Cascades region. These include: 1), MT response functions; 2), fault and stress locations and orientations from the USGS and Oregon DOGAMI active fault databases, the literature, and new LiDAR coverage; 3), major element and isotopic compositions of spring fluids from the USGS database and published/unpublished literature; 4), heat flow from the SMU database; and 5), volcanic distributions from the NAVDAT database. Subsequently, data were processed using state-of-the-art modeling approaches to obtain modern 3D geophysical images, a greatly updated active fault database, estimates of slip and dilatency tendency for fault zones, a re-evaluation of chemical geothermometry, model testing of deep permeability and temperature, a conceptual model of geothermal resources in this region, and common risk segment maps for heat, permeability and prospectivity in the Central Cascades.

3.1 Magnetotelluric Resistivity Structure

Available MT data for the project include 28 legacy EMSLAB profile stations passing from the Coast Range to Mt Jefferson, then jogging around its southern apron and the boundary with the Warm Springs Indian Reservation to just past the town of Madras in the Deschutes Basin (Wannamaker et al., 2014). These are augmented by the long period stations of the Earthscope MT Transportable Array (TA) (Meqbel et al., 2014) providing areal (3D) control for a total of 60 sites. Both station sets are shown in Figure 1. The 3D resistivity image is produced using a new edge finite element algorithm also developed under DOE/GTP support described in detail by Kordy et al (2016a,b). This algorithm simulates topography precisely using deformable hexahedral elements, uses the entire MT tensor set, and exhibits rapid convergence to close data fits because direct matrix solvers are used throughout. A view of the central portion of the finite element mesh used to invert the Central Cascadia MT data is shown in Figure 5. It contains ~1.2M elements with the minimum element width of 1.5 km near center of data array. There were 31 periods ranging from 0.11 through 2560 s at each site (although Earthscope sites did not record to shorter than 4 s) with an error floor of 5% of the average of the two principal elements for

impedance, and 0.03 for tipper. Convergence was monotonic from a 25 ohm-m starting model with a good nRMS fit of 1.6 achieved after 9 iterations and run times of ~31 hours per iteration.

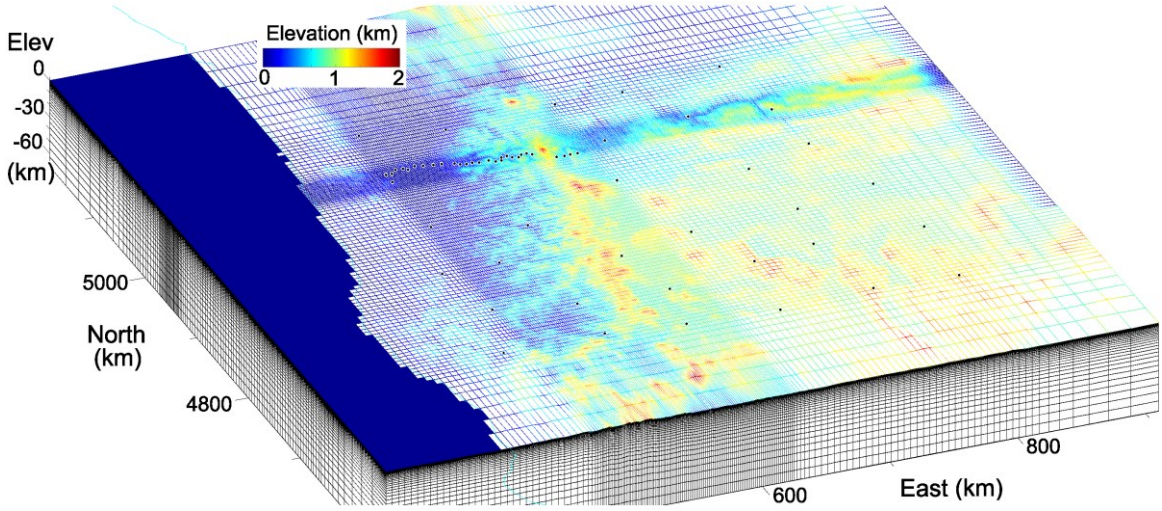

Figure 5: Central portion of finite element mesh for inverting the Central Cascades MT data set. The effects of the Pacific Ocean were explicitly included. Each hexahedral element is a parameter voxel in the inversion. Elevation is represented by color.

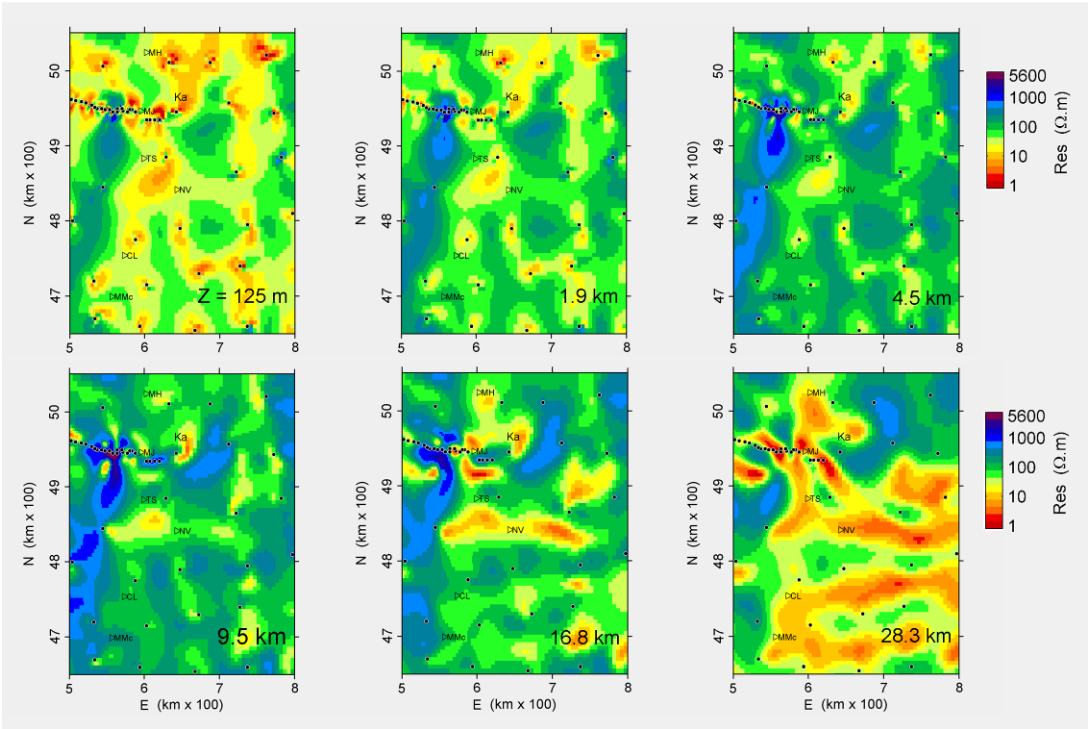

Figure 6: Plan views at various depth levels through central portion of 3D MT inversion model of the EMSLAB profile and Earthscope MT TA stations. Color scale is logarithmic. Localities include Mt Hood (MH), Mt Jefferson (MJ), Three Sisters (TS), Kahneeta Hot Springs (Ka), Newberry volcano (NV), Crater Lake (CL), and Mt McLaughlin (MMc).

Plan views through the 3D resistivity model appear in Figure 6. Starting at lower crustal depths, a series of pronounced E-W oriented conductors underlying the northwestern Basin and Range and terminating under the Cascades volcanic arc become clear. These are similar to Meqbel et al. (2014) using a different algorithm and not including the EMSLAB data. They are interpreted as representing magmatic underplating and fluid release. There is a tendency for the conductive features to project west to the major volcanic centers themselves. Note that there is a concentration of low resistivity from Three Sisters north through Mt Jefferson suggesting a similar concentration of deep magmatic input. This persists to shallow levels, for example 9.5 km. A particularly large, isolated conductor also lies near Kahneeta Hot Springs and persists to shallower levels, though is poorly constrained by only the wide-spaced Earthscope site. At much shallower levels, a few km, patchy low resistivity presumably represents upper crustal sediments and altered volcano-clastic stratigraphy of no high value at this coarse sampling. Nevertheless, the deeper levels of the MT model volume serve as a proxy for large scale magmatic heat input and will be a component of the heat common risk segment map.

3.2 Structural Geology

Structural geology is perhaps the most direct indicator of fluid permeability potential. Structural understanding is substantially upgraded through the analysis of recent and new (2014) LiDAR data coverage (Figure 7a). This coverage is concentrated in the northern portion of our PFA area where cumulative along-strike heat discharge was shown to increase most rapidly. The recent LiDAR coverage of the northern Central Cascades area has been processed to yield more than 1000 new active fault segments. An example of the superior LiDAR resolution is given in Figure 8 for an area of the south flank of Mt Jefferson. The 1 m resolution LiDAR data revealed 22 new faults in this area alone which were not visible in the standard 10 m DEM data. The new fault segments were integrated with the USGS and Oregon DOGAMI active data base for a total population of >16,000 in the overall PFA area (Figure 7b).

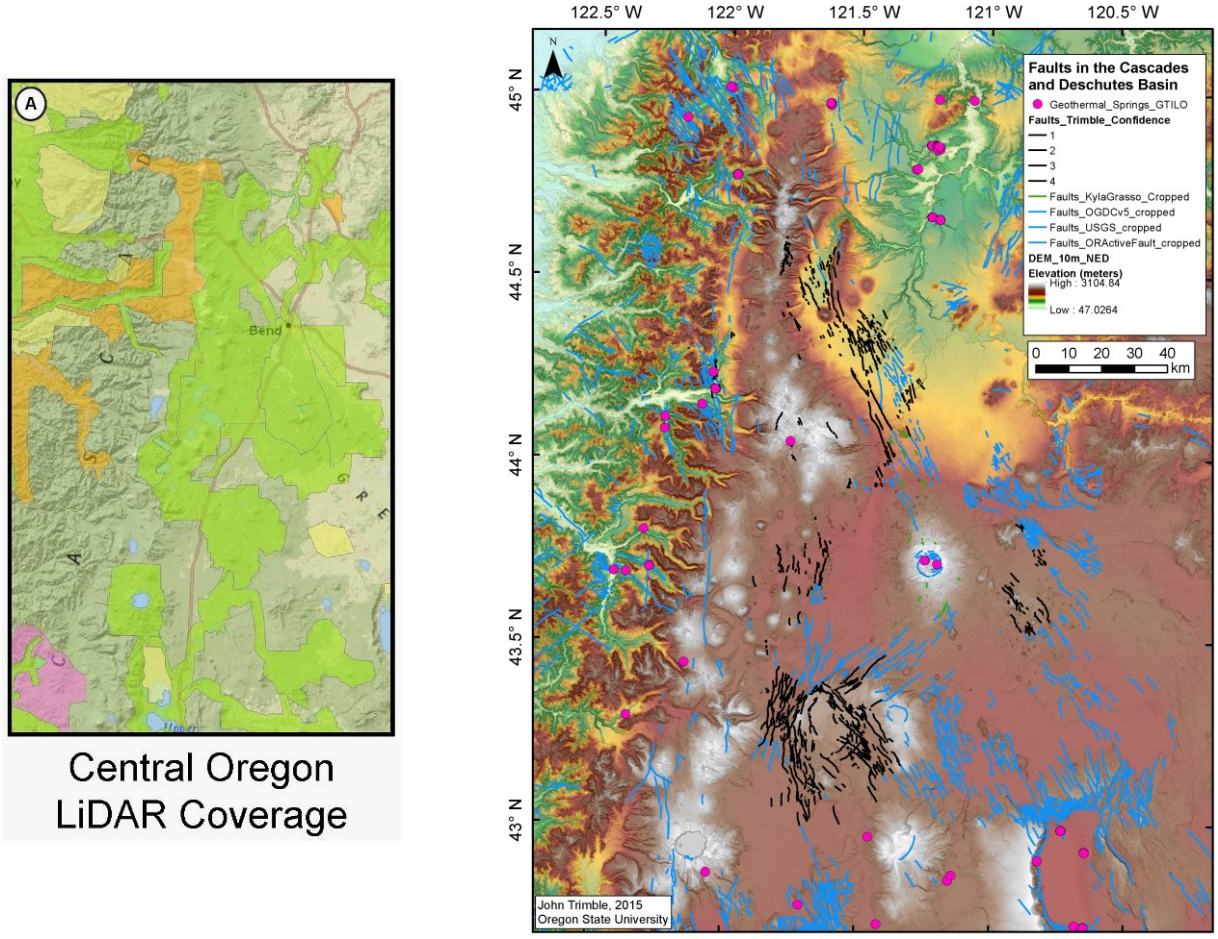

Figure 7: Left (a): LiDAR coverage in the Central Cascades PFA project is represented by the light green and orange shaded regions. The latter coverage was acquired in October 2014. Right (b): Final fault compilation map for the Central Cascades PFA region from USGS and Oregon DOGAMI databases, and new LiDAR interpretation. Select hot springs are Austin (Au), Breitenbush (Br), Kahneeta (Ka), Lower Opal (LO), Belknap (Be), Paulina (Pa) and McCreadie (MC).

Several major features are apparent. First, Mt Jefferson lies in a N-S trending graben whose displacement is diminishing further northward. Hot springs are concentrated along faults of the High-Western Cascades transition west of the arc. However, Breitenbush itself lies in a nexus of N-S and NW-SE trending faults, which is a situation that promotes rock dilatency (e.g. Faulds et al., 2013). Although faulting right in the high Mt Jefferson edifice is locally obscure, the NW-SE trending zone appears to continue through it toward the Sisters fault zone prominent north of Newberry volcano (Figure 12). It is tempting to conclude there is fault zone linkage along this entire length. Finally, there is a complex series of N, NE and NW-trending faults in the Walker Rim area toward the southern portion of our PFA study area.

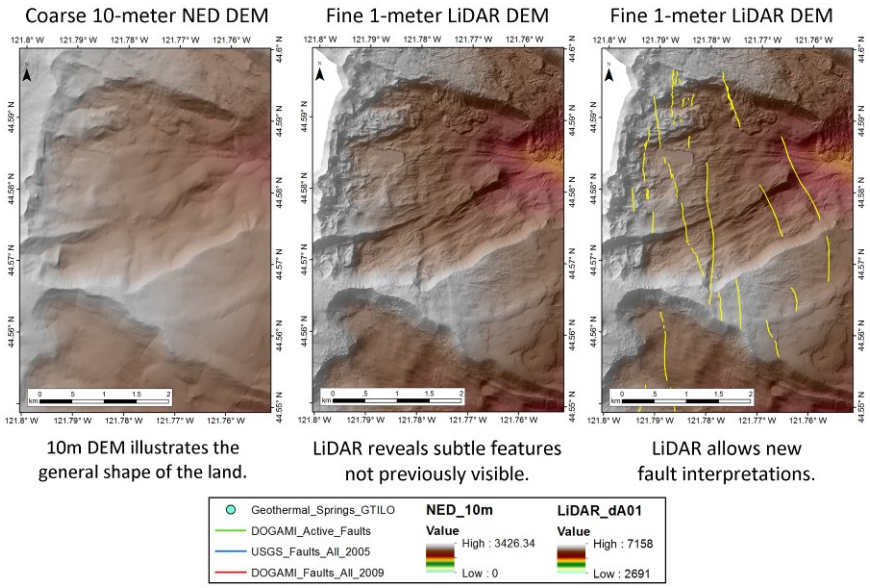

Figure 8: Comparison of fault lineament resolution using standard 10 m DEM and new 1 m LiDAR coverage for a region off the south flank of Mt Jefferson. Analysis by John Trimble of OSU.

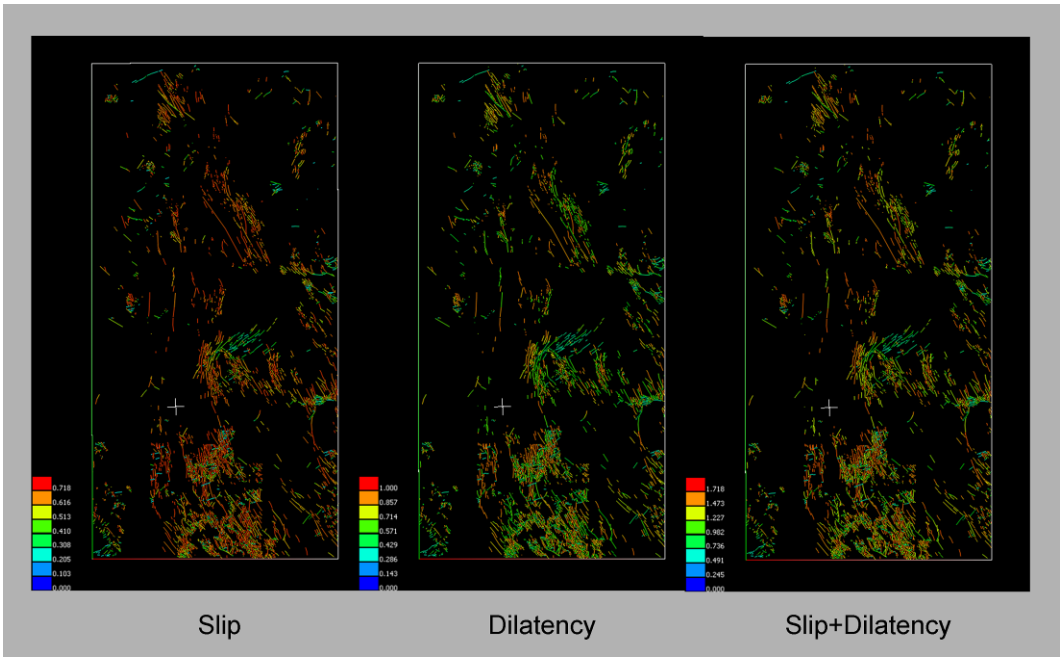

Figure 9: Comparison of fault lineament resolution using standard 10 m DEM and new 1 m LiDAR coverage for a region off the south flank of Mt Jefferson. Analysis by John Trimble of OSU.

For a fault to be permeable, it either must tend to dilate or to slip in the current stress field. The value of dilation is self-evident, and slip should be sufficient as well given that fault asperities should prop the fault open during slip. Slip and dilatency analysis was done for the PFA area using the well-know code 3Dstress (Morris et al., 1996). In the northern portion of the PFA area, the faults are dominantly normal or oblique-normal, whereas they become increasing strike-slip to the south (e.g., Pezzopane and Weldon, 1993). 3Dstress requires an assumption of regional stress state, whose directions were estimated from the literature based on earthquake fo-cal mechanisms, borehole breakouts and vent alignments (Crider et al., 2001; Davatzes and Hickman, 2011; Humphreys and Coblenz, 2007; McCaffery et al., 2013; Pezzopane and Weldon, 1993; Werner et al., 1991). These generally averaged E-W for least principal stress (sigma-3) but also showed variability of order 30 degrees to the NW-SE or SW-NE from that average. Principal stress magnitudes for the regions are poorly determined, so standard magnitudes were assumed at 95, 65 and 25 MPa for sig-1, -2 and -3.

The likeliest representation of slip and dilatency tendency in the project area is depicted in Figure 9 for a regional sigma 3 direction of 080 and a fault dip of 060 (dip direction is immaterial under the Andersonian assumption). One sees that slip tendency is rather strong for both the N-S and NW-SE fault zone orientations, although not so much for NE and E-W orientations such as the northeast side of the Walker Rim area. Dilatency per se is only moderately favorable, but permissible regionally. The sum as expected is intermediate and we conclude that slip events may be more responsible for most permeability creation. Slip tendency reduces if sigma 3 is oriented more NW-SE but increases if sigma 3 is oriented more NE-SW than our central choice. Nevertheless, the fault zones in the region are considered permissible for permeability creation from this standpoint.

3.3 Geochemistry and System Modeling

Figure 9a indicates the limited fluid geochemistry data set with which we have to work, but we are able to make important inferences about subsurface conditions nevertheless. Traditional empirical geothermometry estimates for the springs are compiled in Figure 9b from various published sources (mainly Ingebritsen et al., 1994). Apart from the spike in Na/K inferred tempera-ture at Newberry volcano springs, only two springs (Breitenbush, Shitike) reach 160 C for any of the geothermometers. The remainder tend to lie in the 100-135 C range. Possibly, the low-temperature values could be ascribed to cooling and re-equilibration as the fluids traveled from higher temperature reservoirs. As anticipated, the Na/K temperatures tend to be the highest, presumably reflecting their propensity to lock in the deep temperature conditions encountered and to be relatively immune to dilution by surface waters. Alternatively, these spring waters are simply being heated by rocks of moderate temperatures distal to the large heat sources represented by the volcanic edifices. Taken at face value, existing geothermometry estimates are disappointing in terms of resource implications.

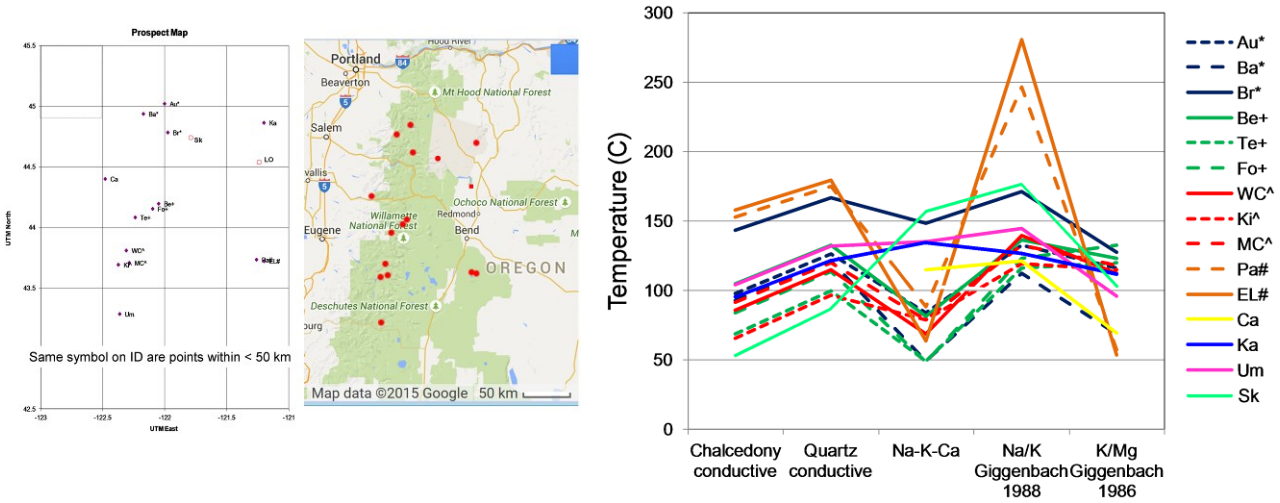

Figure 9: Left (a): Locations of thermal springs with chemical compositions available for interpretation in this PFA project. Acronyms are defined in an upcoming figure with exception of Shitike (Sk) and Lower Opal (LO). Right (b): Compilation of traditional fluid geothermometers for the Central Cascades region. Location of springs in Figure 8. Springs discussed in text include Austin (Au), Breitenbush (Br), Foley (Fo), Belknap (Be), Terwilliger (Te), Paulina (Pa), Kahneeta (Ka), and Shitike (Sk).

An independent check on subsurface temperatures inferred from fluid geochemistry is available from the reaction-based Geo-T algorithm introduced previously (Spycher et al., 2014; Peiffer et al., 2014). Five springs along the High-Western Cascades boundary fault zone were modeled with Geo-T and the results presented in Figure 16. Good intersections of the mineral family equilibrium curves were achieved at temperatures that are near or perhaps slightly above the temperatures inferred from the Na/K geothermometers. A noteworthy exception may be Kahneeta Hot Springs in the backarc where the Geo-T temperature, while quite uncertain due to only moderate convergence, is significantly higher. Otherwise, if important resources exist in the Central Cascades, they are mostly cryptic to present-day, near-surface evidence.

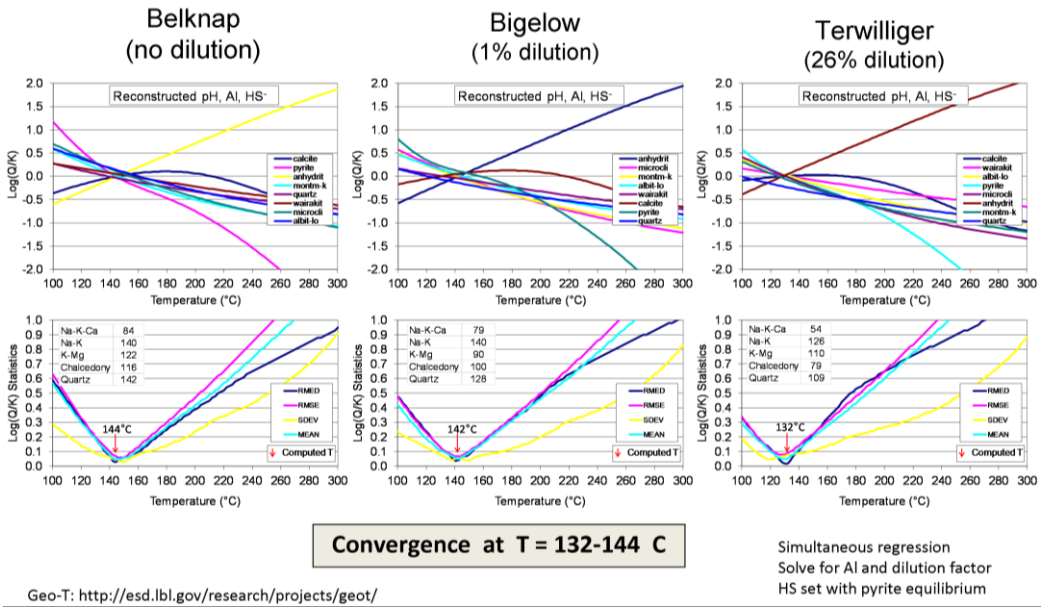

Figure 10: Results of Geo-T modeling calculations for three springs along the High-Western Cascades boundary fault zone directly west of Three Sisters volcanic edifice. Bigelow hot springs is located ~6 km north of Belknap. Spring locations in Figure 9a.

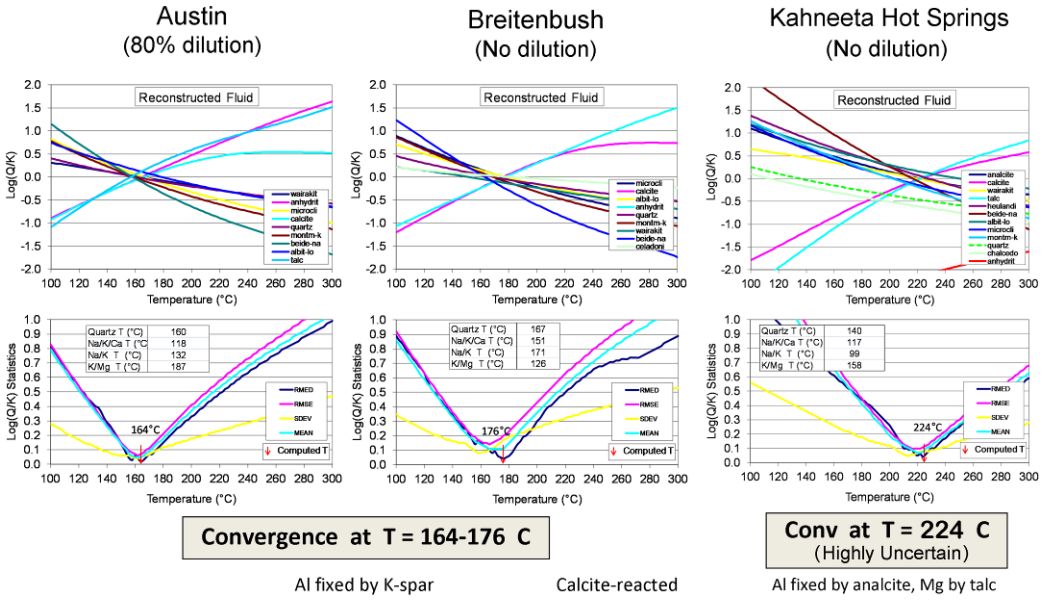

Figure 11: Results of Geo-T modeling calculations for two springs along the High-Western Cascades boundary fault zone northwest of Mt Jefferson volcanic edifice, plus backarc Kahneeta Hot Springs. Spring locations in Figure 9a.

Further clues as to subsurface conditions experienced by fluids in the Central Cascades region are given through balloon plots of select composition components. The main ones we consider are Mg and Cl, and are shown in Figure 12. Mg and Cl concentrations in spring waters are typically taken as an indicator of depth and temperatures to which fluids have circulated in geothermal areas (Nicholson, 1993). Reaction at higher temperatures removes Mg from solution and, if the waters can reach the surface without lower temperature re-equilibration, may indicate high temperature at depth. Most of the spring waters along the High-Western Cascades boundary zone have low Mg suggesting the fluids have seen higher T at depth. Spring geothermometry values here are not economically high, however, so Mg concentrations are not sufficiently positive. A similar case can be made for Cl. In that case also, the correlation between Cl content

and helium R/Ra values suggests basement compositions in addition to volcanoclastics such as early Tertiary marine sediments may be contributing both Cl and radiogenic ^{4}He (van Soest et al., 2004), obscuring the geothermal significance of Cl.

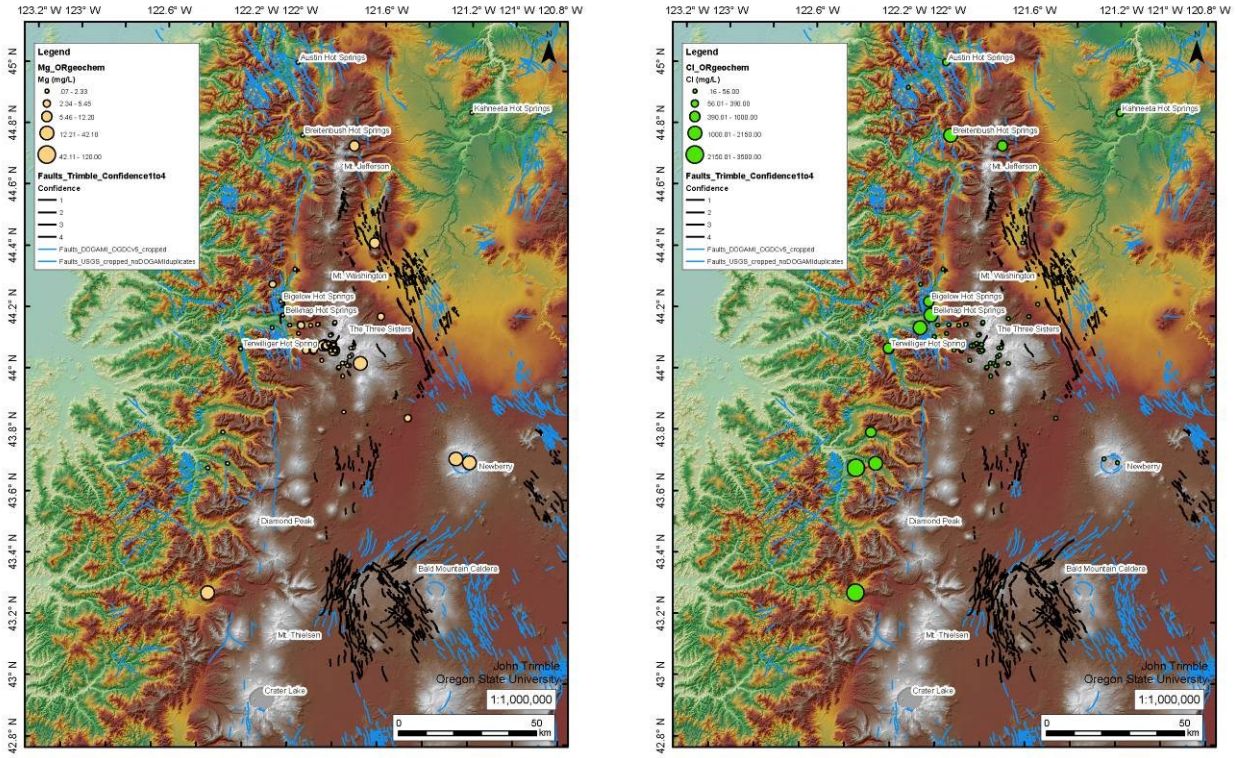

Figure 11: Geochemical balloon plots of Mg (left) and Cl (right) concentration for spring data base of the Central Cascades PFA region, Oregon. Values predominantly from Ingebritsen et al. (1994).

Nevertheless, the strong anomalies in 3He together with magmatic carbon in CO_2 imply that magmatic processes can be nearby and their thermal effects are perhaps close to the surface. This was the conclusion of Evans et al. (2004) for the west flank area of Three Sisters volcanic edifice. However, the anomalous conditions appear to predate the current episode of crustal inflation there, leading Evans et al. to infer that episodes of intrusion may be more common than age and abundance of eruptive events would imply. Given the disappointing characteristics of known springs along the High-Western Cascades boundary transition, perhaps the best hope for the andesite type resource in the Central Cascades lies between the boundary transition and the volcanic edifices.

In the backarc, James et al. (2000) detect measurable proportions of magmatic ^{3}He and ^{13}C in Lower Opal (Figure 9a) and other springs up to 50 km from the High Cascade crest, from which they infer deep fluid circulation and heat mining. Although they point to fluid recharge at the distant crest, our recent experience in the Great Basin (Figure 4) leads us to consider more local, extension related magmatic activity subsurface. To explain the O and H isotopes in the backarc springs would require that a component of the recharge water be older (i.e. Pleistocene) and enter the system under colder conditions as has been suggested for the eastern Great Basin once covered by Pleistocene Lake Bonneville (Simmons et al., 2015).

Both mafic and silicic (andesite to rhyolite) Quaternary volcanic units are represented in the Central Cascades (Wallace, 1991). The latter, representing magmatism that has resided for a considerable time in the upper middle crust, are considered more important than basalts for heat potential. Volcanic products in the northern Central Cascades segment demonstrate that extensional basaltic magma recharge increasingly dominates their evolution, while lack of thinned crust under the arc is a sign that extension and ductile flow balance magmatic underplating (Conrey et al., 2001; Schmidt and Grunder, 2011).

From prior discussion, to find new andesitic systems we would move away from the High-Western Cascades boundary zone due to disappointing experience there and advocate a search closer to the volcanic edifices. It is worth examining whether high-temperature systems may exist closer to the intrusive heat source but are obscured by the shallow hydrological regime (Evans et al., 2004), which would require geophysics and isotopic sampling. Regarding the back-arc, deeper manifestions of hidden extensional systems similar to elsewhere in the Great Basin could exist. Possibly, such structures pass through occurences such as Lower Opal and cryptically to latitudes of Kahneeta Hot Springs and beyond. These again would need similar methods of subsurface detection to prove.

4. COMMON RISK SEGMENT (CRS) MAPPING

Following Following the cataloguing of pertinent available data sets in the Central Cascades, discussion of their individual implications for hydrothermal conditions in the subsurface, and a possible occurrence model for resources in the PFA area, we turn now to quantifying prospective subareas to the extent that probabilistic and multi-criteria decision making (MCDM) approaches allow. One crucial technical aspect is accommodating diverse types of data with varying units and ranges. We approach this through the probability kriging technique in the ArcGIS statistical toolbox. For different data types, we ask what is the probability on a scale of 0 to 1 that the particular data type will exceed a certain threshold considered favorable for a resource, or at least favorable for follow-up investigation. Some of the data are too sparse to allow this. This is particularly true of the geochemical spring sampling which is concentrated along the High-Western Cascades transition. Data such as these are used to support or downplay arguments about resource likelihood in different areas. Following is a presentation of appropriate probability kriged data sets.

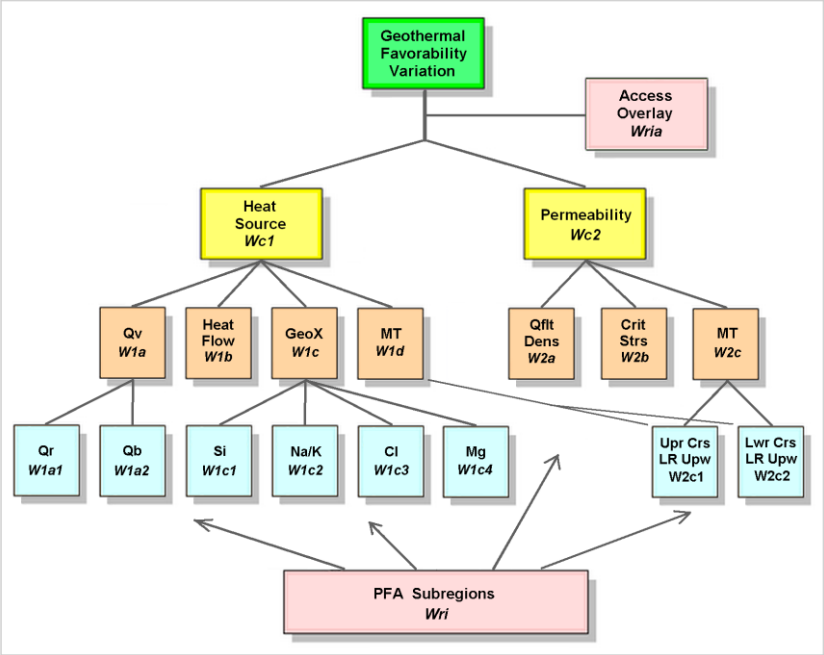

Figure 11: Idealized flow chart in a Multi-Criteria Decision Making (MCDM) framework illustrating factors or criteria considered for prioritizing subregions of the Eastern Great Basin PFA area. If all criteria data were sufficient to be represented in a fully rasterized form, higher level criteria weights such as for heat or permeability result from multiply-sum operations on sub rows. Weights Wijk may be derived from e.g. analytic hierarchy processing (AHP) or directly user specified. Diagram influenced by several publications (e.g., Saaty, 1977, 2008; Teknomo, 2006; Nouri et al., 2013; Boschmann et al., 2014; Wiki, 2015).

4.1 Heat Flow

Heat flow data retrieved from the SMU data base (http://geothermal.smu.edu/gtda/), is presented in Figure 12a according to the probability that flux exceeds 80 mWm-2. In contrast to a simple contour map where two widely spaced points of similar value can lead to an extrapolation of that value across large open spaces, kriged probability represents the uncertainty in defining a threshold where data are sparse or of poor quality. As expected, our confidence that heat flow exceeds 80 mWm-2 is highest near known data which is clustered along the High-Western Cascades boundary faulting and locally at Newberry volcano, Powell Buttes and Pine Mtn. These all are known areas which have been explored and considered of minimal economic promise, although Newberry remains the subject of focused EGS geothermal research. Thus, the known heat flow is unlikely to be given high weight in terms of aggregate heat source for hidden systems in this region.

4.2 Magnetotelluric Conductivity

We synthesize the MT results of Figure 6 by simply inverting to conductivity, which is more linearly related to abundance of fluid or melt, and computing an average from the deep crust to depth of 9.6 km which is probably as shallow as the coarse site spacing generally warrants (Figure 12b). The conductivity structure is transformed to a normalized range by probability kriging and trimmed to the PFA area. Here we see strong conductivity trends focus toward Mt Jefferson near the north end of the study area with lesser concentrations east toward Kahneeta Hot Springs and just south of Three Sisters. There is a strong concentration also east of Newberry toward the Glass Buttes area along the Brothers fault zone although this is outside our PFA area. Two compact conductors west of Mt Jefferson likely are related to eclogitization of the downgoing slab (Wannamaker et al., 2014). Because these anomalies represent concentrations

of melts or high temperature fluids that upwell to higher levels in the crust, MT conductivity can be a component both of the heat source and the permeability favorability criteria.

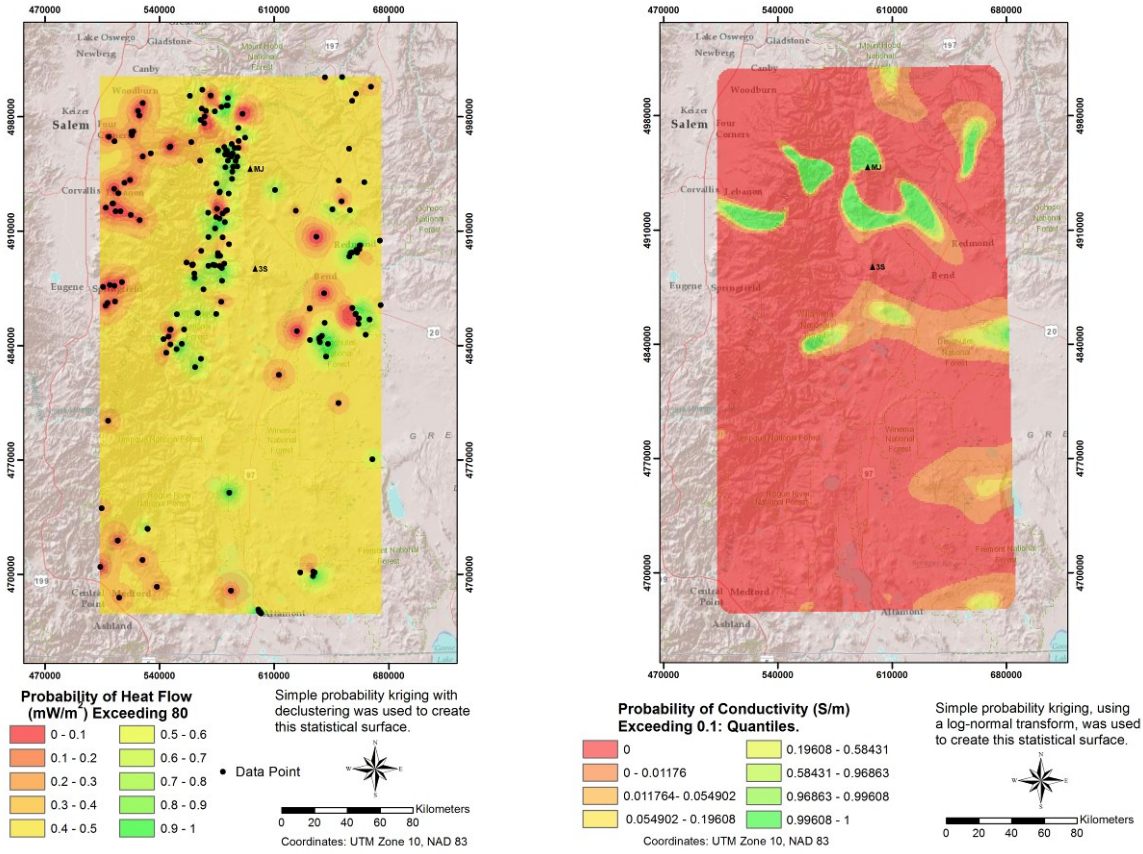

Figure 12: Left (a): Kriging map of probability (0 – 1) that heat flow exceeds 80 mWm-2 in the Central Cascades PFA area. Note that we use green as the color of highest probability (most favorability) and red as the color least favorable. Right (b): Kriging map of probability (0 – 1) that MT conductivity exceeds 0.1 S/m in the Central Cascades PFA area. We use green as the color of highest probability (most favorability) and red as the color least favorable.

4.3 Quaternary Volcanic Intrusives

The third component contributing to estimated heat source potential is presence of Quaternary volcanic intrusives and localized extrusive. Units marked on the map of Walker and McLeod (1991) were divided into basalt and andesite-rhyolite (not shown). The more silicic compositions are considered more favorable as they signify longer term accumulation and hybridization of magmas at mid-crustal levels (e.g., Conrey et al., 2001). In terms of kriged probability, outcrop is simply assigned unity weight, and lack of outcrop is zero. Original outcrop location has been buffered outward by 2 km as a volume of heat influence according to studies of Norton (1991). Obvious silicic outcropping is associated with Mt Jefferson, Three Sisters, Newberry, and Crater Lake. Numerous basalt vents and cones lie directly north of Mt Jefferson, northeast of Sisters, and especially around the Diamond Peaks area in the central part of the PFA region.

4.4 Fault Permeability

The primary quantity available for permeability estimation is fault density, greatly augmented from previous knowledge by the analysis of extensive new LiDAR data. Simple fault density has been output from the ArcGIS platform and is plotted in Figure 13a. This is transformed to kriged probability in the 0 – 1 range and depicted in Figure 13b. The most apparent zones of dense faulting lie in the Breitenbush-Austin area at the northern tip of the study region where N-S and NW-SE fault trends intersect, as well as the extension of NW-SE faulting SE of Mt Jefferson as the Sisters fault zone. There also is denser faulting passing off the project area to the SE into the Glass Buttes region and the Brothers fault zone. High density faulting also occurs around the perimeter of the Walker Rim basaltic field although it does not exhibit intrusives as young as Quaternary (Figure 13b). Finally, there is a large amount of faulting immediately NE of the Klamath Lakes area as the faulting regime transitions from predominantly normal to predominantly strike slip. The slip-dilation tendency analysis discussed with Figure 9 shows roughly equivalent tendencies over all faulted domains except possibly the NE-SW

directed faulting along the northern boundary of the Walker Rim area. Thus, in particular for the northern portion of the PFA area, the areas of dense faulting have reasonable permeability potential.

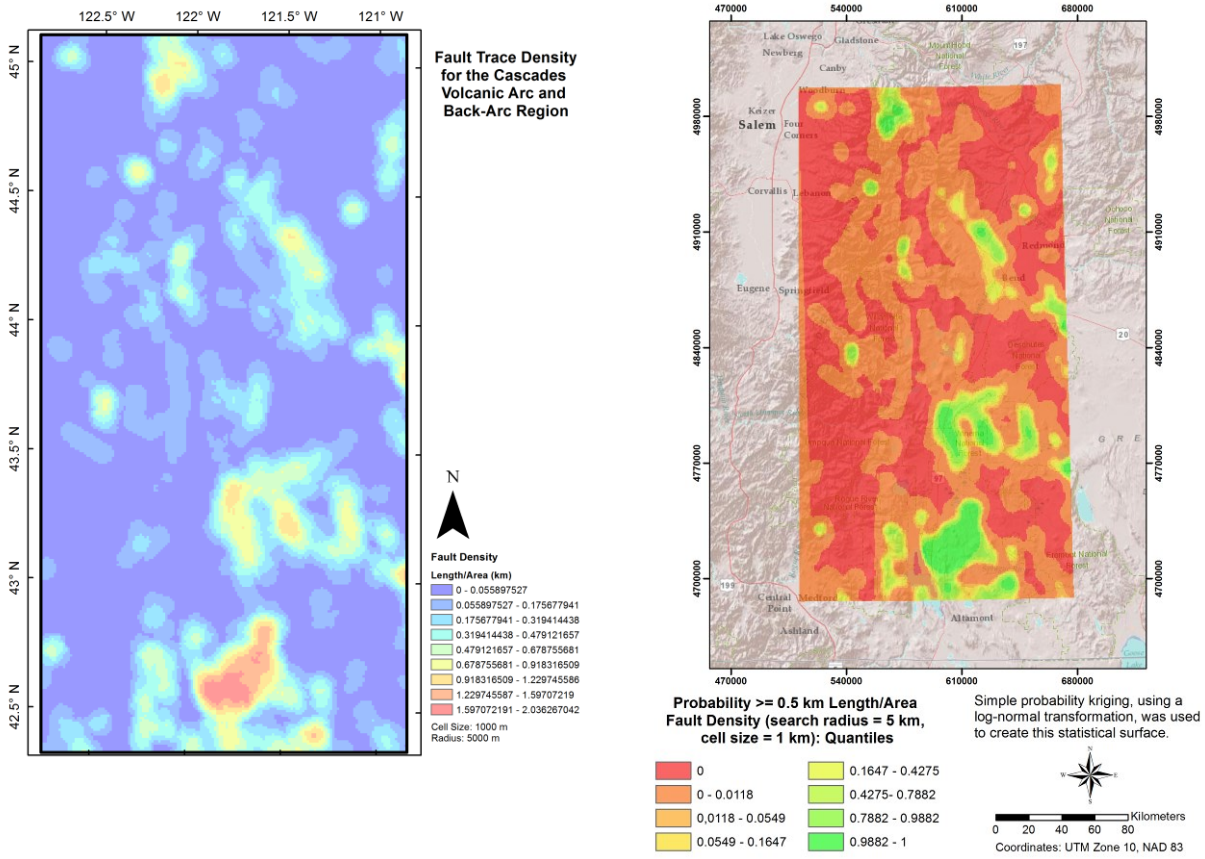

Figure 13: Left (a), fault density in the study area in units of km^{-1}, computed by Ellen Lamont of OSU. Right (b), Kriged probability that fault density exceeds 0.5 km^{-1}.

4.5 Heat and Permeability Favorability Maps

In reference to the MCDM flow chart of Figure 11, heat source potential of the Central Cascades PFA area ideally could be estimated on the basis of Quaternary volcanism, heat flow, fluid geochemistry, and MT geophysics. Prior discussion distinguishes the ideal from reality in terms of which quantities can be combined straightforwardly in such a weighted sum procedure. Heat flow kriged probability is dominated by the locations of data, namely along the High-Western Cascades margin and isolated regions such as Newberry, which either already are considered subeconomic or under separate research study. Thus it is assigned a rather low weight to determine favorability. Fluid geochemical sampling in the project area suffers from a limited number of data points, particularly for the backarc. Consequently, we cannot credibly produce a continuous kriged probability layer of geochemical parameters for the PFA area. Geochemical parameters will have an important concept supporting role especially where other data are sparse as we will discuss shortly. This leaves Quaternary volcanism and MT conductivity as the two main in-dicators which can be treated from a PFA area-wide standpoint. Recognizing the relative impor-tance of the silicic intrusives as discussed, we assign W1a1 = 0.8 and W1b1 = 0.2 for a sum of unity. Subsequently, total heat source potential is derived using the following weightings for Qv, heat flow, and MT conductivity: W1a = 0.3, W1b = 0.15, and W1d = 0.55. Geochemistry W1c is omitted in this formal calculation.

The resulting heat potential map appears in Figure 14a. One observes that heat potential in the vicinity of Mt Jefferson is deemed relatively high due to concentration of silicic volcanic rocks and MT conductivity. Three Sisters area is moderately high potential as is Newberry volcano area, and passing just out of map view is potentially interesting behavior toward Glass Buttes.

For permeability potential, we rely predominantly on fault density with secondary input from MT conductivity. The latter is considered because it is assumed that some permeability is required to allow conductive fluids/melts to upwell. Thus, assigned weights are W2a = 0.65 and W2c = 0.35. Critical stress does not enter the formal calculation as the slip-dilatency tests showed permissible conditions. The resulting permeability potential map appears in Figure 14b.

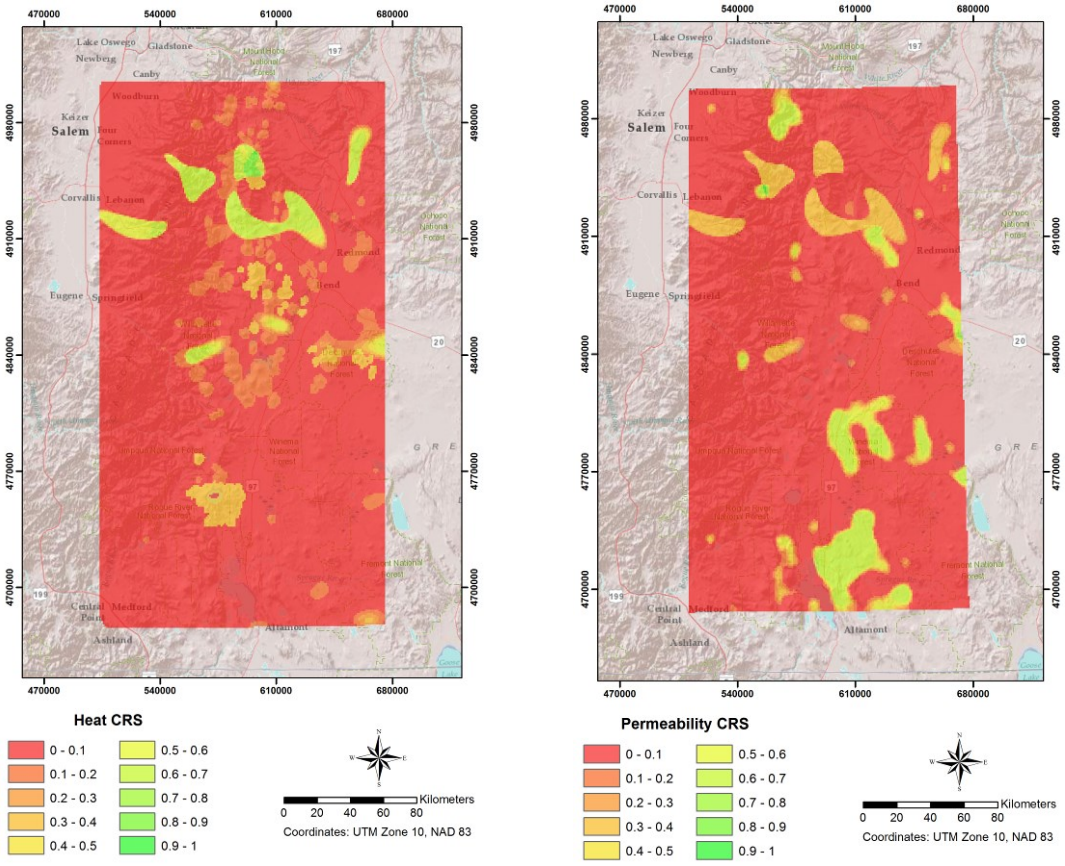

Figure 14: Left (a), Heat potential CRS map of the Central Cascades PFA region. Right (b), Permeability potential CRS map of the Central Cascades PFA region. Weighted sum results are normalized to a full range of unity for display in each map.

4.7 Access and Infrastructure

Land ownership in the PFA area is shown in Figure 15a. The Cascades region is dominated by USDA Forest Service holdings, some of which is wilderness area and will not see development. Development on Forest Service land is not unheard of, with Newberry leases being the best known example. A significant portion east and northeast of Mt Jefferson is land of the Confederated Tribes of Warms Springs (CTWS), including Kahneeta Hot Springs, and access here would need to be negotiated. Transmission lines appear to be sufficiently common and closeby should an economic geothermal resource be identified. A prominent example would be the Detroit Lake hydroelectric dam transmission lines which head to the Portland market and also eastward past Breitenbush Hot Springs and across CTWS land.

4.8 Final Resource and Favorability Mapping

The remaining task of this section is to compute final geothermal favorability by combining heat and permeability potential in a weighted sum, and by taking access and infrastructure into consideration. In this, we assign Wc1 = 0.65 and Wc2 = 0.35 in an effort to make sure heat sources are strongly represented, and to allow for a possibility that EGS resources could be identified even though natural permeability is absent. To account for land access, wilderness areas are overlain and the subjacent favorability blocked out. The final favorability map is shown in Figure 15b, with wilderness exclusion overlay.

This is probably an appropriate point to state that the weights assigned to different criteria in forming the CRS maps are person-defined for the rationales listed above. An alternative sometimes used for defining weights is the analytic hierarchy method (AHP) (Saaty, 1977, 2008; Nouri et al., 2013; Technomo, 2006; Boschmann et al., 2014). In this case, the subcriteria in a row, such as the four in the heat potential row of Figure 2 (Qv, HF, GX, MT), are pairwise compared for relative favorability. The favorability entries are then written into a small matrix (4x4 in the general case here) and the principal eigenvector of that matrix solved. In our case, only three entries are deemed sufficient to define a statistical surface, and of those heat flow was seriously down-weighted due to sparseness and a preponderance of data in non-economic areas. In the case of a 2x2 matrix, the eigenvalue entries equal the original weight entries. The entries in an AHP matrix for an assessment such as this one are as user-defined as the ones we implement here. Our weights are not wide-ranging and experiments with changing relative values yields qualitative changes only in the map views.

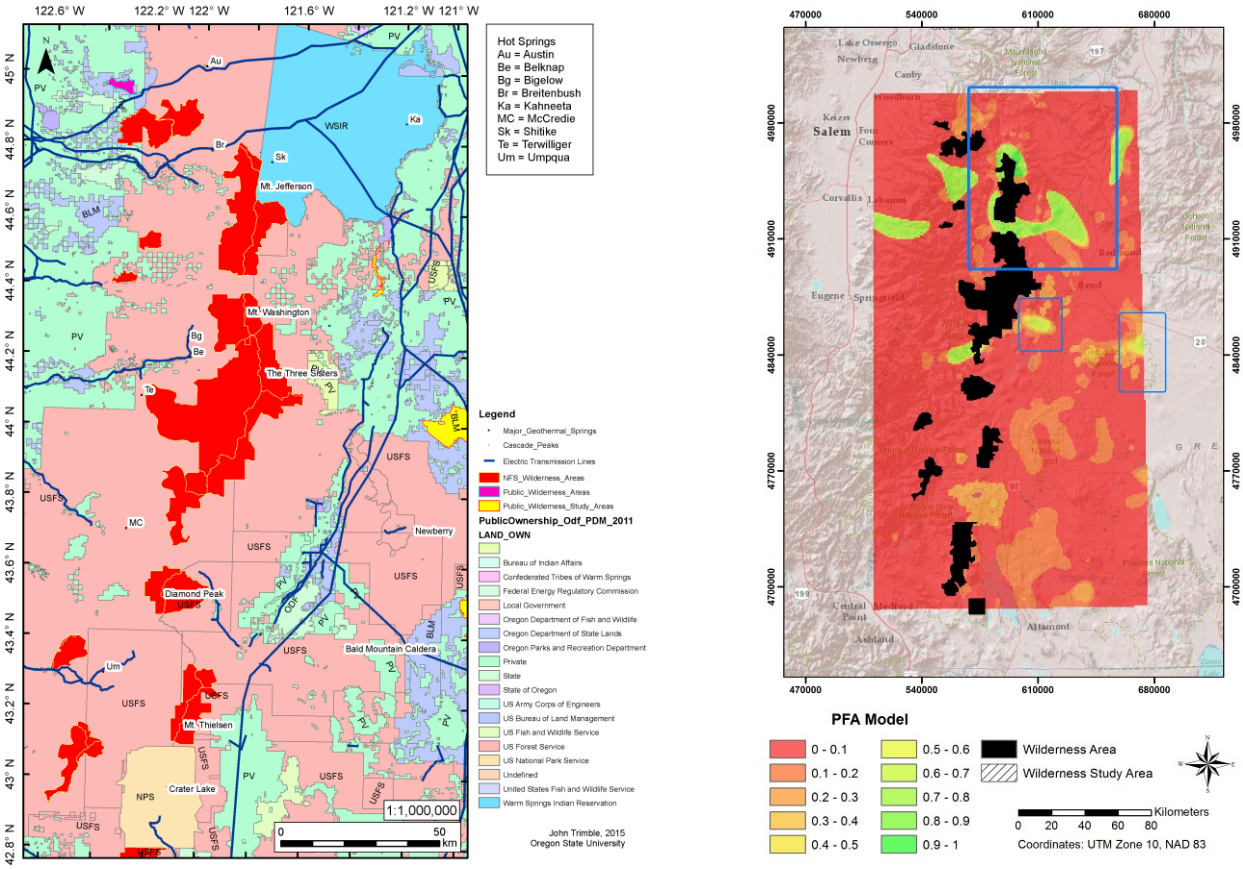

Figure 15a Left (a): Land ownership map and transmission lines for the eastern Great Basin PFA area. Right (b): Geothermal favorability map of the Central Cascades PFA region, including wilderness exclusion and desired followup areas (blue boxes, approx.).

CONCLUSIONS AND RECOMMENDATIONS

The overall favorability map leads us to emphasize the Mt Jefferson area for followup exploration (Figure 15b). The chosen subregion lies where the cumulative heat flow along strike of the Cascades arc is increasing southward most rapidly (Figure 3), implying vigorous intrusive activity. It appears that the Sisters fault zone may continue through the Mt Jefferson edifice and connect into faulting of the Breitenbush-Austin thermal features. Although these springs per say are not of interest, the faulting may provide permeability for systems closer to the magmatism (e.g., Evans et al., 2004).

The backarc area to the east and northeast of Mt Jefferson also is intriguing. Shitike and Kahneeta Hot Springs have interesting geochemical characteristics, there is a distinct crustal scale MT conductor, and the region lies at the terminus of extensional faulting coming in from the south, thus setting up a semi-regional horse-tailing geometry (cf. Faulds et al., 2013). Graphically, this backarc area might appear even more promising than suspected if additional data could be obtained.

The Mt Jefferson-Warms Springs region is advantageous from an access and infrastructure standpoint also. It is closer to power transmission infrastructure than other areas to the south in our PFA regions. Apart from the high crest of the range, official wilderness area is relatively limited here. Lesser priority areas in Figure 15b include a small region immediately southeast of Three Sisters in a area of low resistivity upwelling and mafic vents and cones, and a second one at the eastern limit of our PFA area approaching the Glass Buttes area.

A centerpiece of new acquisition should be of order 150 MT soundings in an approximate grid geometry with average spacing of order 8 km in the larger blue box enclosure of Figure 15b. This is semi-reconnaissance in nature because data are nearly absent although the apparent heat input is significant. Fully 3D inversion is essential. New LiDAR coverage should be acquired in cooperation with the Oregon DOGAMI to seek new active fault populations. This likely would extend northward to cover area around the NW and northern flanks of Mt Jefferson nearly reaching Breitenbush, but could be tailored to results of the MT surveying. New spring geochemical analysis and passive 3He surveying using technology described by Dame et al. (2015) could verify the deep-sourced, high-T nature of

geophysical structures. Given the sparsity of data at present, two or more stages of new data collection likely are needed before play areas pinpointed sufficiently for thermal gradient drilling would be recognized. All stakeholders in the area need to be engaged to bring about efficient and comprehensive evaluation of possible new resources in this area.

ACKNOWLEDGEMENTS

This research was supported by U.S Dept of Energy contract DE-EE0006727. We are grateful to Dr. Michal Kordy for development and advice on application of the 3D MT inversion algorithm HexMT.

REFERENCES

Boschmann, D. E., J. L. Czajkowski, and J. D. Bowman, Geothermal favorability model of Washington State, Washington State Dept. of Natural Resources, **OFR 2014-2**, 20 pp., 2014.

Dame, B. E., D. K. Solomon, W. C. Evans, and S. E. Ingebritsen, Developing a new, passive diffusion sampler suite to detect helium anomalies associated with volcanic unrest: Bulletin of Volcanology, **77**, 17 pp, 2015.

Conrey, R., Trace element and isotopic evidence for two types of crustal melting beneath a High Cascade volcanic center, Mt. Jefferson, Oregon: Contributions to Mineralogy and Petrology, **141**, 710-732, 2001.

Crider, J. G., Oblique slip and the geometry of normal-fault linkage: mechanics and a case study from the Basin and Range in Oregon: Journal of Structural Geology, **23**, 1997-2009.

Davatzes, N. C., and S. H. Hickman, Preliminary analysis of stress in the Newberry EGS well NWG 55-29, Report, AltaRock Energy Inc., Seattle, WA, 2011.

Evans., W. C., M. C. van Soest, R. H. Mariner, S. Hurwitz, S. E. Ingebritsen, C. W. Wicks, Jr., and M. E. Schmidt, Magmatic intrusion west of Three Sisters, central Oregon, USA: the perspective from spring geochemistry: Geology, **32**, 69-72, 2004.

Faulds, J. E., N. H. Hinz, G. M. Dering, and D. L. Siler, The hybrid model – the most accommodating structural setting for geothermal power generation in the Great Basin, western USA: Geothermal Resources Council Transactions, **37**, 3-10, 2013.

Fournier, R. O., Water geothermometers applied to geothermal energy: in Applications of Geochemistry in Geothermal Reservoir Development, UNITAR-UNDP, F. D'Amore, ed., 37-69, 1991.

Fraser, A. J., A regional overview of the exploration potential of the Middle East: a case study in the application of play fairway risk mapping techniques: in Vining, B. A., and S. C. Pickering, eds., Petroleum geology: from mature basins to new frontiers, Proc. 7th Petroleum Geology Conf., Geol. Soc. London, 791-800, 2010.

Henley, R. W., and A. J. Ellis, Geothermal systems ancient and modern: A geochemical review: Earth-Science Reviews, **19**, 1-50, 1983.

Hildreth, W., Quaternary magmatism in the Cascades – geologic perspectives: U.S. Geological Survey Professional Paper **1744**, Reston, VA, 125 pp., 2007.

Humphreys, E. D., and D. D. Coblentz, North American dynamics and western US tectonics: Reviews of Geophysics, **45**, 2007.

James, E. R., M. Manga, T. P. Rose, and G. B. Hudson, The use of temperature and the isotopes of O, H, C, and noble gases to determine the pattern and spatial extent of groundwater flow: Journal of Hydrology, **237**, 100-112, 2000.

Jefferson, A., G. Grant, and T. Rose, Influence of volcanic history on groundwater patterns on the west slope of the Oregon High Cascades: Water Resources Research, **42**, 15 pp., 2006.

Ingebritsen, S. E., and R. H. Mariner, Hydrothermal heat discharge in the Cascade Range, northwestern United States: Journal of Volcanology and Geothermal Research, **196**, 208-218, 2010.

Ingebritsen, S. E., R. H. Mariner, and D. R. Sherrod, Hydrothermal systems of the Cascade Range, north-central Oregon: USGS Professional Paper **1044-L**, 86 pp., 1994.

Kennedy, B. M., and van Soest, M. C., 2007, Flow of mantle fluids through the ductile lower crust: helium isotope trends: Science, **318**, p. 1433-1436.

King, D., and E. Metcalfe, Rift zones as a case for advancing geothermal occurrence models: Proc. 38th Workshop on Geothermal Reservoir Engineering, Stanford, CA, **SGP-TR-198**, 1578-1588, 2013.

Kordy, M. A., P. E. Wannamaker, V. Maris, E. Cherkaev, and G. J. Hill, 3-D magnetotelluric inversion using deformed hexahedral edge finite elements and direct solvers parallelized on SMP computers, Part I: forward problem and parameter jacobians: Geophysical Journal International, **204**, 74-93, 2016a.

Kordy, M. A., P. E. Wannamaker, V. Maris, E. Cherkaev, and G. J. Hill, 3-D magnetotelluric inversion using deformed hexahedral edge finite elements and direct solvers parallelized on SMP computers, Part II: direct data-space inverse solution: Geophysical Journal International, **204**, 94-110, 2016b.

McCaffrey, R., R. W. King, S. J. Payne, and M. Lancaster, Active tectonics of north-western U.S. inferred from GPS-derived surface velocities: Journal of Geophysical Research, **118**, 709-723, 2013.

McKenna, J. R., and D. D. Blackwell, Numerical modeling of transient Basin and Range extensional geothermal systems: Geothermics, **33**, 457-476, 2004.

Meqbel, N. M., G. D. Egbert, P. E. Wannamaker, A. Kelbert, and A. Schultz, Deep electrical resistivity structure of the Pacific NW derived from 3-D inversion of Earthscope USArray magnetotelluric data, Earth and Planetary Science Letters, 10.1016/j.epsl.2013.12.026, 2014.

Moeck, I., G. Kwiatek, and G. Zimmermann, Slip tendency analysis, fault reactivation potential and induced seismicity in a deep geothermal reservoir: Journal of Structural Geology, **31**, 1174-1182, 2009.

Moore, J., R. Allis, M. Nemcok, T. Powell, D. Norman, P. Wannamaker, I. Raharjo, and C. Bruton, The evolution of volcano-hosted geothermal systems based on deep wells from Karaha-Telaga Bodas, Indonesia: American Journal of Science, **308**, doi 10.2475/01.2008.01, 1-48, 2008.

Morris, A., D. A. Ferrill, and D. B. Henderson, Slip-tendency analysis and fault reactivation: Geology, **24(3)**, 275-278, 1996.

Nicholson, K., Geothermal Fluids: Chemistry and Exploration Techniques: Springer, Berlin, 263 pp., 1993.

Norton, D. L., Fluid and heat transport phenomena typical of copper-bearing pluton environments: in, Advances in Geology of the Porphyry Copper Deposits, S. R. Titley ed., The University of Arizona Press, 59-72, 1983.

Nouri, R., P. Afzal, M. Arian, M. Jafari, and F. Feizi, Reconnaissance of copper and gold mineralization using analytical hierarchy process (AHP) in the Rudbar 1:100,000 map sheet, northwest Iran: Journal of Mining and Metallurgy, **49 A (1)**, 9-19, 2013.

Peiffer, L., C. Wanner, N. Spycher, E. L. Sonnenthal, B. M. Kennedy, and J. Iovenitti, Multicomponent vs. classical geothermometry: insights from modeling studies at the Dixie Valley geothermal area: Geothermics, **51**, 154–169, 2014.

Pezzopane, S. K., and R. J. Weldon, Tectonic role of active faulting in central Oregon: Tectonics, **12**, 1140-1169, 1993.

Raharjo, I. B., V. Maris, P. E. Wannamaker, and D. S. Chapman, Resistivity structures of Lahendong and Kamojang geothermal systems revealed from 3-D magnetotelluric inversions, a comparative study: Proc. World Geothermal Congress, Bali, Indonesia, 6 pp., 2010.

Saaty, T. L., A scaling method for priorities in hierarchical structures: Journal of Mathematical Psychology, **15**, 234-281, 1977.

Saaty, T. L., Decision making wiwth the analytic hierarchy process: International Journal of Services Sciences, **1(1)**, 83-98, 2008.

Schmidt, M., E., and A. L. Grunder, Deep mafic roots to arc volcanoes: mafic recharge and differentiation of basaltic andesite at North Sister volcano, Oregon Cascades: Journal of Petrology, **52**, 603-641, 2011.

Schmidt, M., E., A. L. Grunder, and M. C. Rowe, Segmentation of the Cascade Arc as indicated by Sr and Nd isotopic variation among diverse primitive basalts: Earth and Planetary Science Letters, **266**, 166-181, 2008.

Sherrod, D. R., Geology and geothermal resources of the Breitenbush – Austin Hot Springs area, Clackamas and Marion Counties, Oregon: Oregon DOGAMI **OFR O-88-5**, 91 pp., 1988.

Siler, D. L., B. M. Kennedy, P. E. Wannamaker, Regional lithospheric discontinuities as guides for geothermal exploration: Geothermal Resources Council Transactions, **38**, 39-47, 2014.

Simmons, S., S. Kirby, J. Moore, P. Wannamaker, and R. Allis, Comparative analysis of fluid chemistry from Cove Fort, Roosevelt and Thermo: implications for geothermal resources and hydrothermal sys-tems on the east edge of the Great Basin: Geothermal Resources Council Transactions, **39**, 2015.

Spycher, N., L. Peiffer, E. L. Sonnenthal, G. Saldi, M. H. Reed, B. M. Kennedy, Integrated solute multi-component geothermometry: Geothermics, **51**, 113-123, 2014.

Teknomo, K., Analytic hierarchy process (AHP) tutorial: on-line web tutorial, http://people.revoledu.com/kardi/tutorial/AHP/, 2006.

van Soest, M., B. M Kennedy, W. C. Evans, and R. H. Mariner, Mantle helium and carbon isotopes in Separation Creek geothermal springs, Three Sisters area, central Oregon: evidence for renewed volcanic activity or a long term steady state system?: Geothermal Resources Council Transactions, **26**, 361-366, 2002.

van Soest, M. C., W. C. Evans, R. H. Mariner, and M. E. Schmidt, Chloride in hot springs of the Cascade volcanic arc – the source puzzle: in, Water – Rock Interaction Vol. 1; Proceedings of the eleventh international symposium on water – rock interaction (WRI-11), ed. by Wanty, R. B. and R. R. Seal, II, Saratoga Springs, NY, USA,rpt. LBNL-55553, 209-213, 27 June – 2 July, 2004.

Walker, G. W., and N. S. McLeod, Geological map of Oregon: U S Geological Survey map, 1:500K, 2 sheets 1991.

Wannamaker, P. E., W. M. Doerner, and D. P. Hasterok, Integrated dense array and transect MT surveying at Dixie Valley geothermal area, Nevada; structural controls, hydrothermal alteration and deep fluid sources, Proc. 32nd Workshop on Geothermal Reservoir Engineering, Stanford, CA, **SGP-TR-183**, 6 pp, 2007.

Wannamaker, P. E., D. P. Hasterok, J. M. Johnston, J. A. Stodt, D. B. Hall, T. L. Sodergren, L. Pellerin, V. Maris, W. M. Doerner, and M. J. Unsworth, Lithospheric dismemberment and magmatic processes of the Great Basin-Colorado Plateau transition, Utah, implied from magnetotellurics: Geochemistry, Geophysics, Geosystems, **9**, Q05019, doi:10.1029/ 2007GC001886, 36 pp, 2008.

Wannamaker, P. E., V. Maris, D. Hasterok, and W. Doerner, Crustal Scale Resistivity Structure, Magmatic-Hydrothermal Connections, and Thermal Regionalization of the Great Basin: Geothermal Resources Council Transactions, **35**, 1787-1790, 2011.

Wannamaker, P. E., V. Maris, J. Sainsbury, and J. Iovenitti, Intersecting fault trends and crustal-scale fluid pathways below the Dixie Valley geothermal area, Nevada, inferred from 3D magnetotelluric surveying, Proc. 38th Workshop on Geothermal Reservoir Engineering, Stanford, CA, **SGP-TR-198**, 9 pp, 2013a.

Wannamaker, P. E., J. Faulds and B. M. Kennedy, Integrating magnetotellurics, soil gas geochemistry and structural analysis to identify hidden, high enthalpy, extensional geothermal systems, Annual Report to the U.S. DOE/GTP, Contract DE-EE0005514, 13 pp., 2013b.

Wannamaker, P. E., V. Maris, and C. Hardwick, Basin and rift structure of the central Black Rock Desert, Utah, and initial thermal implications, from 3D magnetotellurics: Geothermal Resources Council Transactions, **37**, 41-44, 2013c.

Wannamaker, P. E., R. L. Evans, P. A. Bedrosian, M. J. Unsworth, V. Maris, and R S. McGary, Segmentation of plate coupling, fate of subduction fluids, and modes of arc magmatism in Cascadia, inferred from magnetotelluric resistivity: Geochemistry, Geophysics, Geosystems, **15**, doi:10.1002/2014GC005509, 2014.

Werner, K., E. Graven, T. Berkman, and M. Parker, Direction of maximum horizontal compression in western Oregon determined by borehole breakouts: Tectonics, **10**, 948-958, 1991.

Wisian, K. W., and D. D. Blackwell, Numerical modeling of Basin and Range geothermal systems: Geothermics, **33**, 713-741, 2004.